E-ISSN: 3023-784X

Advanced Radiology and Imaging

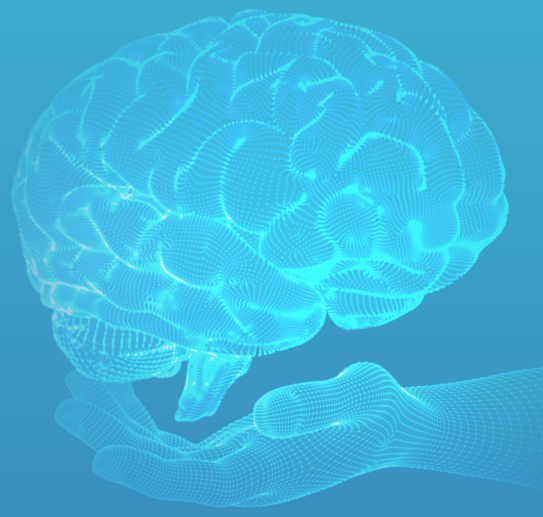

VOLUME 2 / ISSUE 2
AUGUST 2025

galenos Publishing House
ARI
advradiology.org

advradiology.org

Advanced Radiology and Imaging

VOLUME 2 / ISSUE 2
AUGUST 2025

EDITORIAL BOARD

VOLUME 2 / ISSUE 2
AUGUST
2025

Advanced Radiology and Imaging

advradiology.org

Please refer to the journal's webpage (**https://advradiology.org/**) for "**Journal Policy**" and "**Instructions to Authors**".

The editorial and publication process of the Advanced Radiology and Imaging are shaped in accordance with the guidelines of the **ICMJE, WAME, CSE, COPE, EASE,** and **NISO**. The journal is in conformity with the Principles of Transparency and Best Practice in Scholarly Publishing.

Advanced Radiology and Imaging is indexed in **Türkiye Citation Index, IdealOnline, Zenodo, Scilit,** and **Index of Academic Documents.**

The journal is published online.

Owner: Galenos Publishing House

Responsible Manager: Sonay Aydın

Publisher Contact
Address: Molla Gürani Mah. Kaçamak Sk. No: 21/1 34093 İstanbul, Türkiye
Phone: +90 (530) 177 30 97 / +90 (539) 307 32 03
E-mail: info@galenos.com.tr/yayin@galenos.com.tr
Web: www.galenos.com.tr
Publisher Certificate Number: 14521

Publication Date: August 2025
E-ISSN: 3023-784X
International scientific journal published quarterly.

advradiology.org

Advanced Radiology and Imaging

VOLUME 2 / ISSUE 2
AUGUST 2025

CONTENTS

Research Articles

RESEARCH ARTICLE

DOI: 10.4274/AdvRadiolImaging.galenos.2025.02486
Adv Radiol Imaging 2025;2(2):24-31

Effective MRI Practices for Pediatric Patients: Optimizing Imaging Protocols for Safety and Quality

Venkata Raviteja Badveli[1], Ankita G. Cheleng[1], Easwar K. G.[1], Mayurnath Reddy Bedadala[2], Nitishkumar Yeslawath[1]

[1]*Sri Lakshmi Narayana Institute of Medical Sciences, Department of Radiodiagnosis, Puducherry, India*
[2]*University of Miami Faculty of Medicine, Department of Emergency Radiology, Jackson Health System, Miami, USA*

Abstract

Objectives: Magnetic resonance imaging (MRI) is a non-ionizing imaging modality with excellent soft-tissue contrast, ideal for pediatric patients who are more sensitive to radiation. However, challenges such as motion, sedation risks, and anatomical differences require optimized protocols. This study aims to develop and implement pediatric-specific MRI techniques to improve image quality, reduce sedation, and enhance safety. By evaluating current practices and applying advancements like faster sequences and motion correction, the study seeks to establish evidence-based, child-centered protocols for improved diagnostic accuracy and patient outcomes.

Methods: This prospective observational study, conducted in three phases, analyzed existing MRI protocols, developed optimized techniques, and assessed their impact on image quality, safety, and diagnostic accuracy in pediatric patients. Post-implementation surveys evaluated clinician satisfaction. Ethical clearance and informed parental consent were obtained before initiating the study.

Results: This study included 350 pediatric patients, with 200 assessed retrospectively in phase 1 (baseline group) and 150 assessed prospectively following the implementation of optimized protocols in phase 3 (intervention group). The distribution of patients across age groups was as follows: infants (0-2 years): 30% (n=105); young children (3-6 years): 35% (n=123); older children and adolescents (7-18 years): 35% (n=122). There was no significant statistical difference in age or gender distribution between the baseline and intervention groups (p=0.76).

Conclusion: This study reinforces and expands current knowledge on optimized pediatric MRI protocols, demonstrating benefits such as reduced scan duration, improved image quality, and lower sedation rates. These tailored protocols enhance patient safety and diagnostic accuracy while addressing key challenges in pediatric imaging. Incorporating motion correction, fast sequences, and non-pharmacological techniques, the protocols proved clinically effective, supported by positive feedback from radiologists and MRI technicians. Overall, this study highlights the importance of patient-centered, evidence-based pediatric MRI practices.

Keywords: Pediatric MRI, imaging protocol optimization, sedation reduction in MRI imaging, pediatric motion artifact reduction

Introduction

Magnetic resonance imaging (MRI) is a non-ionising diagnostic modality that acquires cross-sectional images and provides excellent soft-tissue contrast. MRI plays a particularly important role in pediatric populations as children are more sensitive to radiation, congenital anomalies, developmental diseases, and oncological conditions.[1] However, children's limited capacity to remain motionless during the scan makes it difficult to apply MRI; therefore, imaging methods must be adjusted to balance patient comfort, image quality, and safety.[2]

Pediatric patients have particular difficulties with MRI procedures due to their distinct physiological and psychosocial traits. Sedation or anesthesia is usually necessary for younger children, particularly those under six years, to provide immobility and reduce anxiety during the treatment.[3] Although sedation reduces motion artifacts and enhances image quality, there are hazards associated with it, such as anesthesia-related side effects and extended recovery periods. To decrease the need for sedation while retaining diagnostic accuracy, imaging techniques must be optimized by employing a comprehensive approach.[3,4]

Additionally, pediatric patients' small body size and different anatomical proportions make the use of specialized equipment and customized imaging parameters necessary. When used on children, standard adult procedures frequently provide less-than-ideal image quality or lengthy scan periods, underscoring the significance of age-

Cite this article as: Badveli VR, Cheleng AG, G EK, Bedadala MR, Yeslawath N. Effective MRI practices for pediatric patients: optimizing imaging protocols for safety and quality. Adv Radiol Imaging. 2025;2(2):24-31

Address for Correspondence: Ankita G. Cheleng MD, Sri Lakshmi Narayana Institute of Medical Sciences, Department of Radiodiagnosis, Puducherry, India
E-mail: freya1996agc@gmail.com ORCID ID: orcid.org/0009-0006-2905-8662
Received: 29.05.2025 Accepted: 22.07.2025 Epub: 14.08.2025 Published: 29.08.2025

appropriate protocol design.[1,5] Faster imaging sequences, motion correction algorithms, and child-specific coils are examples of hardware and software advancements that could improve the effectiveness and quality of pediatric MRI.[4]

Optimizing MRI protocols for pediatric patients is crucial for various reasons. These include safety concerns, especially with regard to the use of gadolinium-based contrast agents, thermal effects, and acoustic noise levels. The high decibel levels generated by MRI equipment make pediatric patients more vulnerable to hearing loss, and the thermal effects from extended scanning can pose further hazards.[5] Furthermore, the use of gadolinium-based contrast agents in children has raised difficulties like gadolinium retention in the brain and other tissues, necessitating adherence to careful application and the most recent safety regulations.[4,5]

The objective of this study is to develop and implement optimized MRI protocols for pediatric patients, balancing diagnostic image quality with patient safety and comfort. This involves analyzing current imaging practices to identify inefficiencies, evaluating advancements in imaging techniques and protocol modifications, and assessing their impact on image quality and diagnostic accuracy. The study aims to establish standardized best practices for pediatric MRI, with particular attention to sedation practices and contrast agent usage, ultimately improving patient outcomes and streamlining clinical workflows.

Methods

This study was approved by the Sri Lakshmi Narayana Institute of Medical Sciences Institutional Ethical Committee approval (decision no: IEC/C-P/37/2022, date: 07.07.2022). Informed consent was obtained from the parents of all the participating patients.

A prospective, observational approach was used in this study to create and execute MRI procedures that were optimized for pediatric patients. The study was conducted in three phases: phase 1, involved analyzing current protocols; phase 2, involved developing optimized techniques; and phase 3, involved assessing the effects of these techniques on image quality, safety, and diagnostic accuracy. A post-implementation survey of radiologists and MRI technicians was also conducted to reveal the level of satisfaction with the optimized protocols in terms of improved workflow, image quality, and confidence in the protocols' ability to minimize sedation requirements without compromising diagnostic accuracy.

Study Population: The study population consisted of 150 pediatric patients aged 0 to 18 years referred for MRI examinations at a tertiary care hospital. Patients were grouped into three age categories for analysis and protocol development (Table 1):

1. Infants (0-2 years),
2. Young children (3-6 years),
3. Older children and adolescents (7-18 years),
4. Exclusion criteria included contraindications to MRI (e.g., ferromagnetic implants) or conditions that precluded safe sedation (e.g., severe respiratory disorders).

Phase 1: Analysis of Existing Protocols

1. Data collection: Retrospective data were collected from 200 MRI scans conducted in the past year (Figures 1-3). This included information on:

- Scan parameters (sequence type, scan duration, field strength)
- Sedation or anesthesia usage
- Image quality assessment reports
- Safety incidents or complications

2. Evaluation metrics: Protocol efficiency was assessed based on:

- Average scan duration
- Incidence of motion artifacts
- Sedation requirements
- Image quality was graded by two independent radiologists using a standardized scoring system (1=poor, 5=excellent).

3. Gap analysis: Protocol inefficiencies, including extended scan times, frequent need for sedation, and suboptimal image quality, were identified.

Phase 2: Development of Optimized Protocols

1. Protocol modifications: Optimized protocols were developed by integrating the following strategies:

- Sequence selection: Use of rapid imaging sequences (e.g., T1-weighted spoiled gradient echo, single-shot fast spin echo) to reduce scan duration.
- Motion correction technologies: Implementation of advanced software solutions such as Periodically Rotated Overlapping Parallel Lines with Enhanced Reconstruction and parallel imaging.
- Age-specific parameters: Adjustment of field of view (FOV), slice thickness, and repetition time (TR) based on patient age and body size. Smaller children require a smaller FOV and thinner slices, while larger adults need larger FOV and thicker slices. Shorter TRs are generally preferred for faster imaging in older patients to minimize motion artifacts. Longer TRs are needed for younger patients to improve signal-to-noise ratio (SNR).
- Acoustic noise reduction: Use of noise-suppressing techniques, like silent MRI sequences and hearing protection devices. These sequences are designed to minimize the intensity and frequency of gradient coil switching, thus reducing the noise generated.

Table 1. Demographics and study population

Age group	Baseline group n (%) (n=200)	Intervention group n (%) (n=150)	Total n (%) (n=350)
Infants (0-2 years)	60 (30%)	45 (30%)	105 (30%)
Young children (3-6 years)	70 (35%)	53 (35%)	123 (35%)
Older children and adolescents (7-18 years)	70 (35%)	52 (35%)	122 (35%)

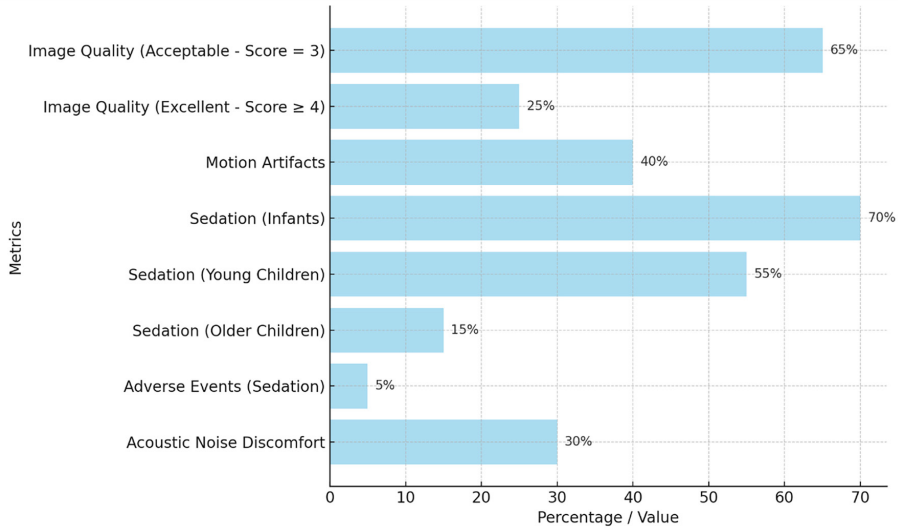

Figure 1. Baseline group metrics for pediatric MRI

MRI: Magnetic resonance imaging

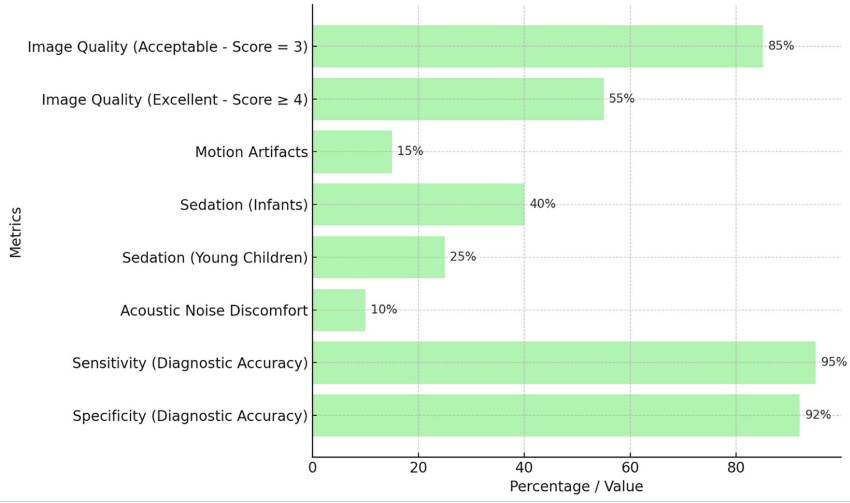

Figure 2. Intervention group metrics for pediatric MRI

MRI: Magnetic resonance imaging

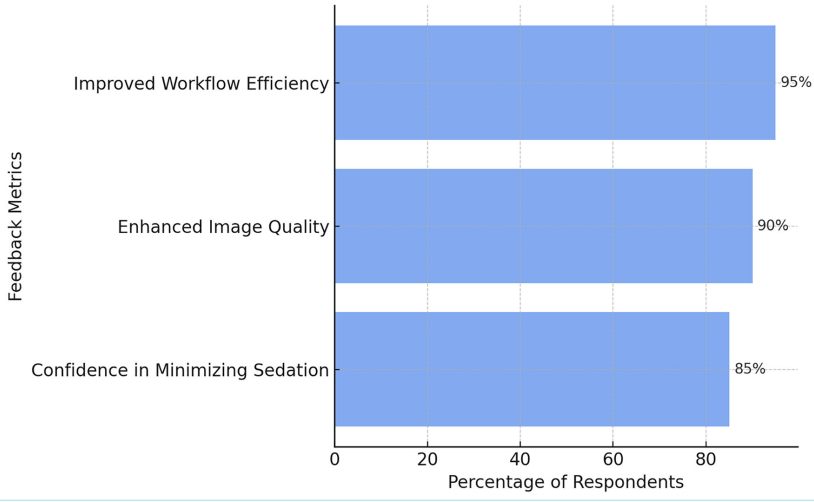

Figure 3. Feedback from radiologists and technicians

2. Hardware optimization pediatric-specific coils (e.g., head, torso, and extremity coils) were used to improve the SNR and accommodate smaller anatomical structures.
3. Reduction in sedation rates: Non-pharmacological techniques, such as child life specialist consultations, visual aids, and mock scanner sessions, were incorporated to reduce anxiety and improve compliance.

Phase 3: Evaluation of Optimized Protocols

1. Study intervention: The optimized protocols were applied to 150 pediatric patients over six months. Data were prospectively collected on:

- Image quality
- Sedation usage
- Scan duration
- Safety outcomes (e.g., adverse events)

2. Image quality assessment: Two board-certified radiologists, blinded to protocol type, independently evaluated image quality using the same standardized scoring system as in phase 1.
3. Comparison with baseline: Pre- and post-implementation data were compared to assess the impact of optimized protocols (Table 2).
4. Diagnostic accuracy: Radiological reports were reviewed to determine whether the optimized protocols affected diagnostic accuracy. Sensitivity and specificity metrics were calculated for selected pathologies (e.g., tumors, developmental abnormalities).

Statistical Analysis

All data were analyzed using Statistical Package for the Social Sciences version 26 (IBM Corp., Armonk, NY, USA). Continuous variables (e.g., scan duration) were expressed as mean ± standard deviation and assessed for normality using the Shapiro-Wilk test. Pre- and post-implementation data were compared to assess the impact of optimized protocols using statistical tests such as paired t-tests for continuous variables, and chi-square tests for categorical outcomes. Paired t-test determined if there is a statistically significant difference between the means of two related groups, while chi-square tests were employed for categorical variables such as sedation rates. Statistical significance was set at $p<0.05$.

Results

This study included 350 pediatric patients, with 200 assessed retrospectively in phase 1 (baseline group) and 150 assessed prospectively following the implementation of optimized protocols in phase 3 (intervention group). The distribution of patients across age groups was as follows:Infants (0-2 years): 30% (n=105), young children (3-6 years): 35% (n=123), Older children and adolescents (7-18 years): 35% (n=122). There was no significant statistical difference in age or gender distribution between the baseline and intervention groups ($p=0.76$)

Phase 1: Analysis of Existing Protocols

Scan duration: The mean scan duration for the baseline group was 45±10 minutes. Longer scan times were observed in younger children (<6 years), primarily due to higher rates of motion artifacts and interruptions.

Image quality: Image quality scores in the baseline group were suboptimal, with 65% of scans rated as acceptable (score=3) and only 25% rated as excellent (score ≥4). Motion artifacts were the leading cause of poor image quality, occurring in 40% of scans for infants and young children.

Sedation use: Sedation was required in 70% of infants and 55% of young children, compared to 15% of older children and adolescents. Adverse events related to sedation occurred in 5% of cases, including minor complications such as prolonged recovery time and nausea.

Safety metrics: Acoustic noise-related discomfort was reported in 30% of patients, and no thermal injuries or significant safety incidents were documented.

Phase 3: Evaluation of Optimized Protocols (Figures 1, 2, Table 2)

Scan duration: The mean scan duration in the intervention group was significantly reduced to 25±5 minutes ($p<0.001$). The reduction was most pronounced in younger children because optimized sequences and motion correction techniques minimized the need for repeated scans.

Image quality: Image quality scores improved significantly in the intervention group, with 85% of scans rated as acceptable (score=3) and 55% rated as excellent (score ≥4) ($p<0.001$). Motion artifacts were reduced in 15% of scans conducted on infants and young children due to the use of faster sequences and improved immobilization techniques.

Sedation use: Sedation rates decreased by 30% overall. Only 40% of infants and 25% of young children required sedation in the intervention group, compared to 70% and 55%, respectively, in the baseline group ($p<0.001$). Non-pharmacological techniques, including mock scanner sessions and child life specialist consultations, were cited as key factors in reducing sedation requirements.

Safety metrics: Acoustic noise-related discomfort was reduced to affecting only 10% of patients due to the use of noise-suppressing

Table 2. Comparison of key metrics between baseline and intervention group

Metric	Baseline group	Intervention group	p value
Mean scan duration (minutes)	45±10	25±5	**<0.001**
Image quality (excellent, %)	25%	55%	**<0.001**
Sedation rate (overall, %)	50%	20%	**<0.001**
Motion artifacts (overall, %)	40%	15%	**<0.001**
Acoustic discomfort (%)	30%	10%	**<0.01**
Diagnostic sensitivity (%)	94%	95%	0.76
Diagnostic specificity (%)	91%	92%	0.85

techniques and hearing protection devices ($p<0.01$). No adverse events related to thermal effects or contrast agent use were observed. The judicious use of gadolinium-based contrast agents, guided by updated protocols, ensured safety without compromising diagnostic accuracy.

Diagnostic accuracy: Radiological interpretations confirmed that optimized protocols did not compromise diagnostic accuracy. Sensitivity and specificity for detecting key pathologies (e.g., tumors, developmental anomalies) were 95% and 92%, respectively, comparable to baseline metrics.

A post-implementation survey of radiologists and MRI technicians revealed a high level of satisfaction with the optimized protocols: 95% of respondents reported improved workflow efficiency. 90% of radiologists noted enhanced image quality in pediatric scans. 85%, expressed confidence in the protocol's ability to minimize sedation requirements without compromising diagnostic accuracy (Figure 3).

Discussion

The findings of this study align with and extend the current understanding of optimized MRI protocols in pediatric patients, as discussed in previous research. By focusing on scan duration, image quality, sedation rates, and safety metrics, this study validates earlier findings while offering new insights into practical improvements in pediatric MRI.

The significant reduction in scan duration from 45±10 minutes to 25±5 minutes is similar to findings from prior studies that have emphasized the role of faster imaging sequences and advanced motion correction technologies. The use of parallel imaging techniques and single-shot fast spin echo sequences greatly shortened scan times in pediatric populations, especially for younger children who are more susceptible to motion artifacts, as studied by Kuperman et al.[3] Our results corroborate these findings, as optimized sequences not only minimized interruptions but also improved overall workflow efficiency. Additionally, better patient comfort is linked to faster scans, which is crucial in healthcare settings with limited resources. The decrease in the average scan time in our investigation is consistent with earlier results highlighting the significance of sophisticated imaging methods. Meissner et al.[6] demonstrated that motion correction techniques dramatically reduced the requirement for repeated scans, particularly in younger children who are more likely to move. Similarly, the effectiveness of rapid imaging sequences in obtaining quicker and more effective scans in pediatric patients was also noted by Gewirtz et al.[7]

With acceptable scans rising from 65% to 85% and outstanding scans rising from 25% to 55%, the intervention group's image quality dramatically improved. This improvement is in line with research by Kanal et al.[2] that showed how motion correction methods and age-specific coils greatly improve the diagnostic image quality in pediatric MRI. These investigations revealed increased SNRs and decreased motion artifacts, especially in younger children, which is consistent with our findings. Maintaining diagnostic accuracy, particularly when identifying subtle developmental defects or diseases, depends on this improvement in image quality. The enhanced image quality is in line with research by Vecchiato et al.[8], who found that motion correction algorithms and age-specific MRI coils greatly improve diagnostic imaging, especially in children who are difficult to work with. Our study's improved image quality (85% assessed as acceptable and 55% as excellent) is also consistent with Sun et al.[9], who showed how contemporary imaging technologies enhance children's diagnostic clarity and SNRs.

In our study, sedation rates dropped by 30%, and non-pharmacological measures, including child life specialist involvement and mock scanner sessions, were crucial. Bhargava et al.[1] found that lowering the use of sedation in pediatric MRI improves patient safety without sacrificing diagnostic quality, which supports our study. Our research supports this by showing that these types of interventions help children feel less anxious and become more physically active. Nonetheless, a noteworthy constraint identified in earlier research, which is relevant to our results, is the need for skilled workers to execute these methods. Future studies are needed to investigate such approaches for putting these interventions into practice in various healthcare environments. Mock scanner sessions and other non-pharmacological methods have been shown to be successful in reducing anxiety, thereby requiring less sedation.[10]

The decrease in acoustic noise-related discomfort from 30% to 10% is consistent with the study conducted by Alibek et al.[5], who highlighted the significance of hearing protection and noise-suppressing devices in pediatric MRI. Furthermore, our study found no adverse events associated with the use of contrast agents, which is supported by Karabulut[4], who emphasized that the hazards of gadolinium retention in the brain and other tissues are reduced when gadolinium-based contrast agents are used sparingly. The necessity of a patient-centered approach in pediatric imaging is shown by the incorporation of these safety measures. Our results of decreased acoustic noise discomfort (from 30% to 10%) are consistent with research showing how crucial noise-dampening devices are in MRI. A similar study was done by Gewirtz et al.[7] to lessen patient suffering, especially in younger populations. Furthermore, our study found no negative effects from gadolinium-based contrast agents which supports recommendations made by Sun et al.[9] about the prudent and safe use of these agents.

Our study's diagnostic accuracy showed excellent results, with sensitivity and specificity of 95% and 92%, respectively, which were equivalent to baseline measurements. This result is in line with Kanal et al.[2], who showed that even with shorter scan times and lower sedation rates, optimized protocols do not impair diagnostic accuracy. Maintaining strong diagnostic performance is essential to prevent clinical outcomes from being deteriorated safety and efficiency. The high diagnostic sensitivity (95%) and specificity (92%) maintained in our study are consistent with findings from Kinner et al.[10], who reported a sensitivity of 93.6% and specificity of 94.3% without sacrificing safety. This outcome demonstrates how well-suited optimized pediatric MRI techniques are for use in clinical settings.

Rapid MRI procedures minimize sequence duration and quantity, eliminate contrast and anesthetic administration, and optimize workflow. For the assessment of acute abdominal pain, head trauma, cerebral dysfunction, and nontraumatic neurologic symptoms, rapid diagnostic techniques have been implemented.[11]

Since minimizing patient motion is necessary to provide high-quality images, research has concentrated on cutting scan times through the use of strategies, including compressed sensing, rapid sequencing, and single-shot acquisition. Despite these developments, minimum scanning times frequently exceed two minutes, necessitating sedation or anesthesia in children to avoid motion artifacts.[12]

General anesthesia or sedation is frequently used to scan young children, allowing for high-quality scans and a consistent and easy workflow.[13] Regrettably, there are numerous disadvantages associated with the use of sedation and general anesthesia at pediatric MRI, including (a) increased cost, (b) longer examination and recovery times, (c) longer wait times due to limited anesthesia availability, and (d) a higher risk to a child's neurodevelopment for short-term and possibly long-term complications of the sedative and anesthetic agents.[14]

Various measures have been tested to reduce the risks associated with sedation in MRI. Careful selection of drug and dose, along with improved monitoring during sedation, are required because of the current limitations of imaging techniques and the introduction of nonpharmacologic approaches.[15] Patient monitoring during procedural sedation appears to rely mainly on peripheral oxygen saturation, and only one-third of the respondents reported that heart rate, blood pressure, or respiratory rate was regularly monitored.[16] Sedation guidelines recommend the maintenance of physiological homeostasis by regularly monitoring the oxygenation rate, heart rate, ventilation rate, and blood pressure.[17]

Assessing neurocognitive development in children is complex due to its multifactorial nature. However, evidence from a recent large-scale, multi-national randomized controlled trial with follow-ups at 2 and 5 years indicates that brief, single episodes of sedation in young pediatric patients are generally safe.[18]

Consequently, there has been substantial interest in developing new MRI strategies to minimize acquisition time and thereby decrease the use, depth, and duration of sedation during pediatric MRI procedures.[19] Despite much enthusiasm for the use of these MRI time reduction techniques in pediatric patients, the diagnostic accuracy of many of them has yet to be fully established in this population, particularly for the assessment of subtle or small lesions. Further characterization of the diagnostic reliability and limitations of these fast MRI strategies will form an essential next step as their clinical use becomes more widespread.[20]

Although our study showed notable increases in sedation rates, scan duration, and picture quality, the findings may not be applicable elsewhere due to the need for trained staff to provide non-pharmacological therapies. Furthermore, while multicenter studies, like those by Kuperman et al.[3], have shown variation in the adoption of optimum procedures among institutions, our study concentrated on a single-center population. Future research should be done to address these discrepancies. Increased SNR and shorter scanning times are two benefits of using stronger field strength, magnets, which will help children who are prone to movement.[21]

Our findings (Figures 4-7) validate and extend the results of previous studies, emphasizing the value of tailored pediatric MRI protocols. By reducing scan duration, enhancing image quality, and minimizing sedation requirements, these protocols improve patient safety and diagnostic outcomes. However, addressing the implementation challenges, particularly in resource-limited settings, remains a key area for future research.

Study Limitations

- Small sample size.
- Participants were not prepared for the mock examination.
- Children with cognitive impairment were not included in the study.

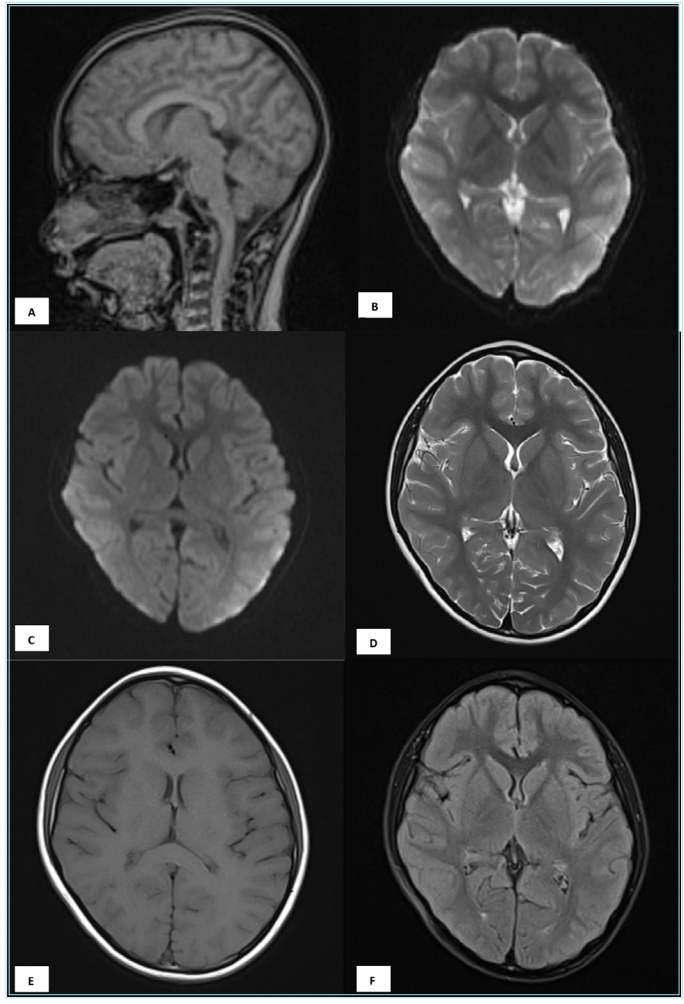

Figure 4. (A-F) Normal MRI brain images in a 10-year-old male child

MRI: Magnetic resonance imaging

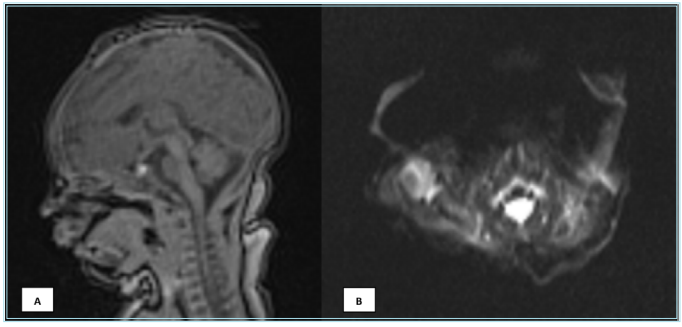

Figure 5. (A, B) MRI images in a newborn male child showed movement artifacts

MRI: Magnetic resonance imaging

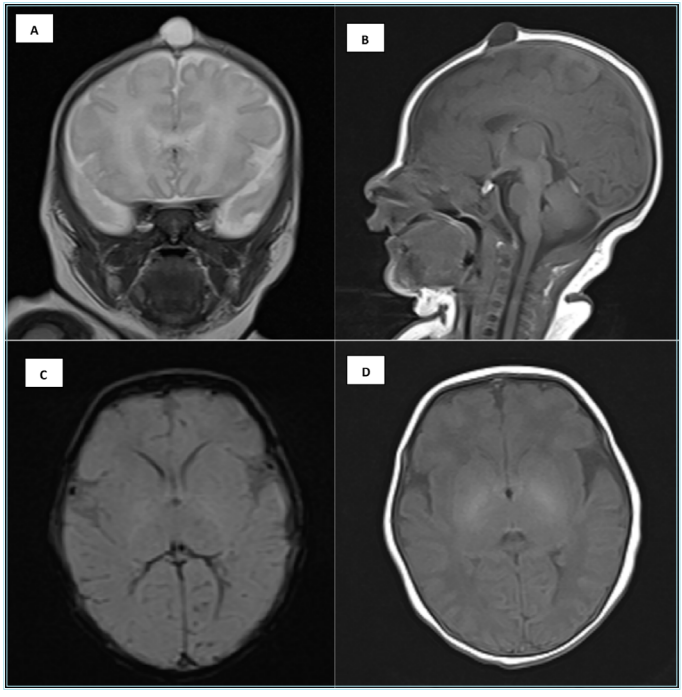

Figure 6. (A-D) MRI images in the same child obtained using tailored protocols showed an anterior fontanelle inclusion cyst and brain parenchyma with better resolution

MRI: Magnetic resonance imaging

Conclusion

The substantial advantages of using MRI protocols that are optimized for pediatric patients are illustrated by this study. These procedures use motion correction technologies, non-pharmacological therapies, and rapid imaging sequences to solve persistent issues in pediatric imaging. However, challenges such as the reliance on trained personnel and the need for resource-intensive technologies must be addressed to ensure scalability across diverse healthcare settings. Future research should explore the integration of artificial intelligence and automated systems to further enhance the quality, safety, and accessibility of pediatric MRI.

Ethics

Ethics Committee Approval: This study was approved by the Sri Lakshmi Narayana Institute of Medical Sciences Institutional Ethical Committee approval (decision no: IEC/C-P/37/2022, date: 07.07.2022).

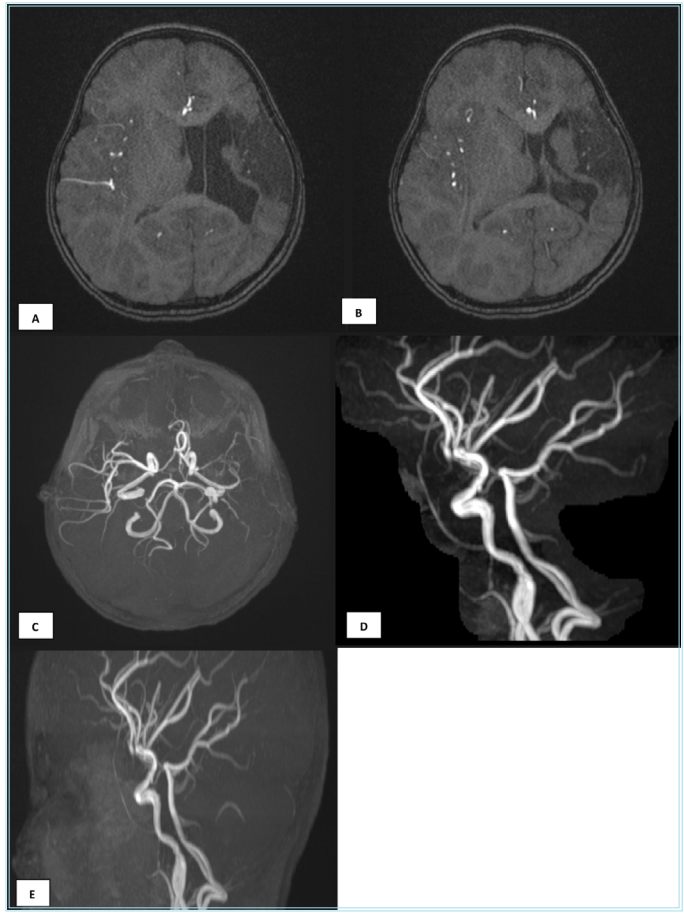

Figure 7. (A-E) MRI (3D-TOF) images in a 3-year-old child with chronic infarct showed encephalomalacic changes that follow CSF signal intensity on all sequences with surrounding gliosis involving the left fronto-parieto-temporal lobes, left thalamus, and basal ganglia. Ex-vacuo dilatation of ipsilateral lateral ventricle and prominent adjacent sulcal spaces are seen. Reconstructed images show hypointensities in the involved vessels. Features are likely suggestive of Wallerian degeneration, secondary to chronic infarct

MRI: Magnetic resonance imaging, TOF: Time-of-flight, CSF: Cerebrospinal fluid

Informed Consent: Informed consent was obtained from the parents of all the participating patients.

Footnotes

Authorship Contributions

Concept: M.R.B., N.Y., Design: M.R.B., N.Y., Data Collection or Processing: V.R.B., A.G.C., E.K.G., Analysis or Interpretation: V.R.B., A.G.C., Literature Search: V.R.B., Writing: V.R.B.

Conflict of Interest: No conflict of interest was declared by the authors.

Financial Disclosure: The authors declared that this study received no financial support.

References

1. Bhargava R, Hahn G, Hirsch W, et al. Contrast-enhanced magnetic resonance imaging in pediatric patients: review and recommendations for current practice. Magn Reson Insights. 2013;6:95-111.

2. Expert Panel on MR Safety; Kanal E, Barkovich AJ, et al. ACR guidance document on MR safe practices: 2013. J Magn Reson Imaging. 2013;37:501-30.
3. Kuperman JM, Brown TT, Ahmadi ME, et al. Prospective motion correction improves diagnostic utility of pediatric MRI scans. Pediatr Radiol. 2011;41:1578-82.
4. Karabulut N. Gadolinium deposition in the brain: another concern regarding gadolinium-based contrast agents. Diagn Interv Radiol. 2015;21:269-70.
5. Alibek S, Vogel M, Sun W, et al. Acoustic noise reduction in MRI using silent scan: an initial experience. Diagn Interv Radiol. 2014;20:360-3.
6. Meissner TW, Walbrin J, Nordt M, Koldewyn K, Weigelt S. Head motion during fMRI tasks is reduced in children and adults if participants take breaks. Dev Cogn Neurosci. 2020;44:100803.
7. Gewirtz JI, Skidmore A, Smyth MD, et al. Use of fast-sequence spine MRI in pediatric patients. J Neurosurg Pediatr. 2020;26:676-81.
8. Vecchiato K, Egloff A, Carney O, et al. Evaluation of DISORDER: retrospective image motion correction for volumetric brain MRI in a pediatric setting. AJNR Am J Neuroradiol. 2021;42:774-81.
9. Sun J, Li H, Li J, et al. Improving the image quality of pediatric chest CT angiography with low radiation dose and contrast volume using deep learning image reconstruction. Quant Imaging Med Surg. 2021;11:3051-8.
10. Kinner S, Pickhardt PJ, Riedesel EL, et al. Diagnostic accuracy of MRI versus CT for the evaluation of acute appendicitis in children and young adults. AJR Am J Roentgenol. 2017;209:911-9.
11. Chan KS, McBride D, Wild J, Kwon S, Samet J, Gibly RF. A rapid MRI protocol for the evaluation of acute pediatric musculoskeletal infections: eliminating contrast and decreasing anesthesia, scan time, and hospital length of stay and charges. J Bone Joint Surg Am. 2024;106:700-7.
12. Uramatsu M, Takahashi H, Barach P, et al. Improving pediatric magnetic resonance imaging safety by enhanced non-technical skills and team collaboration. Brain Dev. 2025;47:104311.
13. Heuvelink A, Saini P, Taşar Ö, Nauts S. Improving pediatric patients' magnetic resonance imaging experience with an in-bore solution: design and usability study. JMIR Serious Games. 2025;13:55720.
14. Jaimes C, Murcia DJ, Miguel K, DeFuria C, Sagar P, Gee MS. Identification of quality improvement areas in pediatric MRI from analysis of patient safety reports. Pediatr Radiol. 2018;48:66-73.
15. Harrington SG, Jaimes C, Weagle KM, Greer MC, Gee MS. Strategies to perform magnetic resonance imaging in infants and young children without sedation. Pediatr Radiol. 2022;52:374-81.
16. Paul B. Pediatric sedation outside of the operating room: an international multispecialty collaboration. New York: Springer; 2011:429-44.
17. Weiss M, Vutskits L, Hansen TG, Engelhardt T. Safe anesthesia for every tot - the SAFETOTS initiative. Curr Opin Anaesthesiol. 2015;28:302-7.
18. Kozak BM, Jaimes C, Kirsch J, Gee MS. MRI techniques to decrease imaging times in children. Radiographics. 2020;40:485-502.
19. Artunduaga M, Liu CA, Morin CE, et al. Safety challenges related to the use of sedation and general anesthesia in pediatric patients undergoing magnetic resonance imaging examinations. Pediatr Radiol. 2021;51:724-35.
20. Zhang T, Chowdhury S, Lustig M, et al. Clinical performance of contrast enhanced abdominal pediatric MRI with fast combined parallel imaging compressed sensing reconstruction. J Magn Reson Imaging. 2014;40:13-25.
21. Saunders DE, Thompson C, Gunny R, Jones R, Cox T, Chong WK. Magnetic resonance imaging protocols for paediatric neuroradiology. Pediatr Radiol. 2007;37:789-97.

RESEARCH ARTICLE

DOI: 10.4274/AdvRadiolImaging.galenos.2025.55264
Adv Radiol Imaging 2025;2(2):32-35

Evaluation of Circle of Willis Variations Using 1.5 Tesla Time-of-flight Magnetic Resonance Angiography

Koray Bingöl, Taner Kösetürk, Mukadder Sunar

Erzincan Binali Yıldırım University Faculty of Medicine, Department of Anatomy, Erzincan, Türkiye

Abstract

Objectives: The circle of Willis (COW) is an arterial ring located at the base of the brain that connects the internal carotid and vertebral arteries through anastomotic branches. This circle includes two anterior cerebral arteries (ACA) connected by the anterior communicating artery (AComA) in the anterior part; two posterior cerebral arteries (PCA) linked to the carotid system via the posterior communicating arteries (PCom), along with the basilar artery in the posterior part. Collateral circulation in the COW is important in maintaining adequate cerebral blood flow in cases of obstructive arterial diseases. This study aimed to reveal the frequency of each COW variation detected on magnetic resonance imaging (MRI) time-of-flight images.

Methods: This retrospective study included of 410 adult patients who underwent brain MRI due to symptoms such as headache, dizziness, ormemoryloss. Anterior and posterior segments of the COW (A1, AComA, PCom, P1) were evaluated separately. Vessel segments with a diameter smaller than 1 mm were considered hypoplastic. Vascular diameters of the COW were measured through the axial plane, perpendicularly to the elongation of the artery and 3 mm from the vessel origin. When the vascular segment is too short, the middle part of the artery is measured.

Results: Of the 410 individuals, 176 were male and 234 female, with a mean age of 41.2±12.7 years. A complete, symmetric COW was observed in 118 cases (28.8%). The most common variations were: - PCom hypoplasia: right 23.1%, left 18.6% - PCom aplasia: right 9.7%, left 7.6% - fetal PCA: unilateral 11.2%, bilateral 4.6% - azygos ACA: 0.7% - basilar artery fenestration: 0.7% - persistent trigeminal artery: 0.2%. There were no statistically significant differences in the prevalence of variation between sexes ($p>0.05$).

Conclusion: COW exhibits significant anatomical variability between individuals. Awareness of these anatomical patterns is important in clinical decision-making, influencing treatment strategies and risk assessment.

Keywords: Manyetic resonance imaging, manyetic resonance angiography anatomical variation, Willis polygon

Introduction

The circle of Willis (COW) (circulus arteriosus cerebri) is an arterial ring located at the base of the brain that connects the internal carotid and vertebral arteries through anastomotic branches (Figure 1). This circle includes two anterior cerebral arteries (ACA) connected by the anterior communicating artery (AComA) in the anterior part, and two posterior cerebral arteries (PCA) linked to the circle via the posterior communicating arteries (PCom), along with the basilar artery in the posterior part.[1] In normal anatomy, a complete and symmetric configuration-called the "typical" COW-is rare; a functionally complete arterial ring is not commonly observed in the general population.[2] In autopsy series, only about 21% of cases exhibit a fully symmetric and complete circle.[3] Most individuals have at least one segmental variation such as hypoplasia or aplasia. These normal anatomical variations are considered the result of differences during embryological development and are commonly encountered even in healthy individuals.[4,5]

The clinical relevance of COW variations is significant. A complete circle supports collateral flow in cases of carotid or vertebrobasilar artery occlusion. An incomplete or anomalous circle may lead to inadequate perfusion of brain regions, increasing the risk of ischemic stroke.[6] For, example, PCom aplasia may reduce vertebrobasilar contribution to the PCA territory, leading to vertebrobasilar insufficiency.[7] Conversely, the presence of a fetal PCA indicates PCA perfusion from the internal carotid system, which may increase the risk of infarction in the PCA territory in cases of unilateral carotid stenosis.[8] Similarly, the absence of AComA or ACA A1 segments limits collateral flow and may compromise anterior cerebral circulation.[9]

Understanding these variations is vital for clinical procedures such as endovascular interventions, aneurysm clipping, carotid artery stenting, and stroke management. For example, in the surgical treatment of AComA aneurysms, knowledge of cross-flow patterns through the circle is critical.[10] Thus, the configuration of the COW is essential in planning cerebrovascular interventions.

Cite this article as: Bingöl K. Kösetürk T, Sunar M. Evaluation of circle of Willis variations using 1.5 Tesla time-of-flight magnetic resonance angiography. Adv Radiol Imaging. 2025;2(2):32-35

Address for Correspondence: Koray Bingöl MD, Erzincan Binali Yıldırım University Faculty of Medicine, Department of Anatomy, Erzincan, Türkiye
E-mail: koray.bingol@erzincan.edu.tr ORCID ID: orcid.org/0009-0007-9927-3576
Received: 22.07.2025 Accepted: 18.08.2025 Published: 29.08.2025

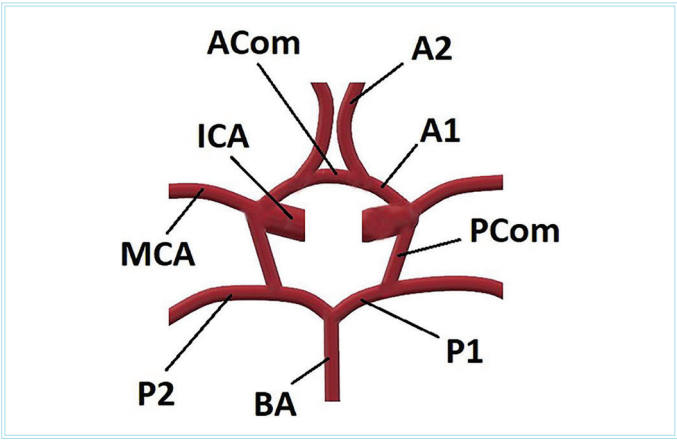

Figure 1. A schema will be used to present the different types of COW and to indicate the differences between the variances better

Acom: Anterior communicating artery, PCom: Posterior communicating artery, P1: pre communicating segment of posterior cerebral artery, P2: Post communicating segment of posterior cerebral artery, ICA: İnternal carotid artery, A1: Pre communicating segment of anterior cerebral artery, A2: Post communicating segment of posterior cerebral artery, MCA: Middle cerebral artery

This study aimed to reveal the frequency of each COW variation detected using TOF images of MRI in a population that had no previous cerebrovascular pathology.

Methods

The study was conducted with approval from the Erzincan Binali Yıldırım University Non-Interventional Clinical Research Ethics Committee (decision no: 2025-14/05, date: 24.07.2025). This retrospective study included time-of-flight (TOF) magnetic resonance angiography (MRA). The study analyzes images of 410 adult patients who underwent brain MRI between January 2022 and March 2024 due to symptoms such as headache, dizziness, or memory loss.

To avoid the possible effects of other vascular diseases on vessel calibers of the COW, the medical records of these patients have been scanned. Four patients with left ICA occlusion, one patient with basilar artery aneurysm, one patient with significant (>50%) right ICA stenosis, one patient with ACom aneurysm, one patient with vascular malformation, one patient with subdural effusion, and one patient with sizeable cerebral hematoma were also excluded from the study. MR angiography images with artifacts hindering interpretation due to motion (cannot remain stable during the examination or patients with dyskinesia) and other imaging artifacts (due to ferromagnetic intracerebral aneurysm clips, etc.) were excluded from the study (n=8).

All imaging was performed without contrast using a 1.5 Tesla scanner (Siemens Magnetom Aera, Germany).

A 16-channel standard head coil was used in each patient. The 3D-TOF images were handled with technical parameters as follows: repetition time: 24 ms, echo time: 7.15 ms, flip angle: 25°, slice thickness: 0.6 mm, field of view: 243×256 mm, and matrix size: 0.4×0.4×0.6 mm^3. The imaging time was approximately 7 min 18 s.

Anterior and posterior segments of the COW (A1, AComA, PCom, P1) were evaluated separately. Hypoplasia was defined as a vessel diameter of less than 1 mm.

Statistical Analysis

Analyses were made using IBM Statistical Package for the Social Sciences 25 statistical software. The normal distribution of continuous variables was checked with Shapiro-Wilk and Kolmogorov-Smirnov tests. In comparisons between two independent groups of male and female participants, the independent samples t-test was used when normal distribution was met, and the Mann-Whitney U test was used otherwise. In 2x2 categorical variable comparisons (frequency >5), Pearson chi-square test was used; if the expected value was between 3 and 5, Yates' corrected chi-square test was used; and if the expected value was less than 3, Fisher's exact test was used. The level of statistical significance was accepted as $p<0.05$.

Results

Of the 410 individuals, 176 were male and 234 female, with a mean age of 41.2±12.7 years. A complete, symmetric COW was observed in 118 cases (28.8%). The most common variations were: - PComhypoplasia: right 23.1% (n=94), left 18.6% (n=76) - PComaplasia: right 9.7% (n=39), left 7.6% (n=31) - fetal PCA: unilateral 11.2% (n=45), bilateral 4.6% (n=18) -AComAaplasia: 2.1% (n=8) - ACA A1 hypoplasia: right 4.1% (n=16), left 2.8% (n=11) - ACA A1 aplasia: 3.4% (n=13) - ACA trifurcation: 2.4% (n=9) - azygos ACA: 0.7% (n=3) -basilar artery fenestration: 0.7% (n=3) – persistent trigeminal artery: 0.2% (n=1). (Tables 1, 2) (Figures 2, 3)

There were no statistically significant differences in variation prevalence between sexes ($p>0.05$).

Discussion

The findings of this study are largely consistent with previous literature. For example, Chen et al.[11] reported a 27% prevalence of complete circles in a Chinese population. The fetal PCA rate in our study was 15.8%, similar to Koshy et al.[12], that who reported 18.3%. ACA segment variations were relatively low (3-6%), suggesting preserved anterior collateral flow in most individuals.[13]

Table 1. Prevalance of anterior COW variants

Anterior variant type	Number of patients (n)	Percentage (%)
AcomAaplasia	8	2.1
ACA A1 hypooplasia right	16	4.1
ACA A1 hypooplasia left	11	2.8
ACA A1 aplasia	13	3.4
ACA trifurcation	9	2.4
Azygos ACA	3	0.7

COW: Circle of Willis, ACA: Anterior cerebral arteries, Acom: Anterior communicating artery

Table 2. Prevalance of posterior COW variants

Posterior variant type	Number of patients (n)	Percentage (%)
PcomAplasia right	39	9.7
PcomAplasia left	31	7.6
PcomHypoplasia right	94	23.1
PcomHypoplasia left	76	18.6
Fetal PCA ipsilateral	45	11.2
Fetal PCA bilateral	18	4.6

COW: Circle of Willis, PCA: Posterior cerebral arteries, Pcom: Posterior cerebral arteries

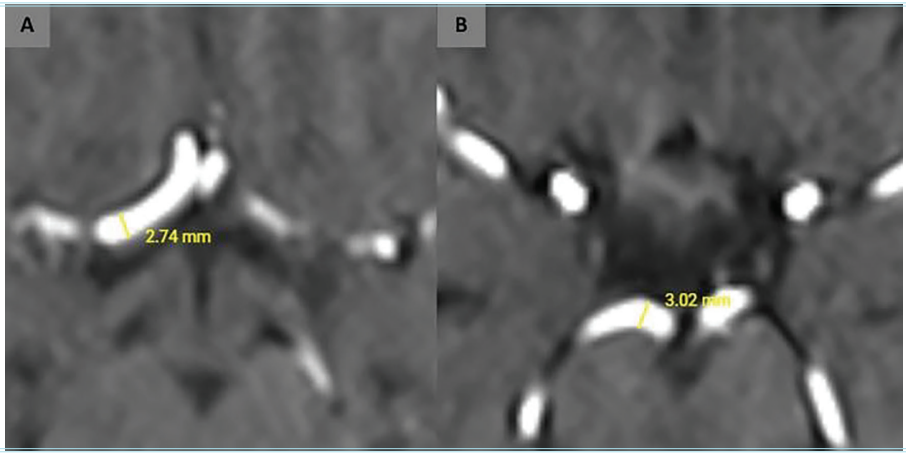

Figure 2. The measurements of vascular diameters of the right A1 segment (A) and right P1 segment (B) are presented. Axial MR images with ×400 magnification were used to measure the vessel calibers

MR: Magnetic resonance

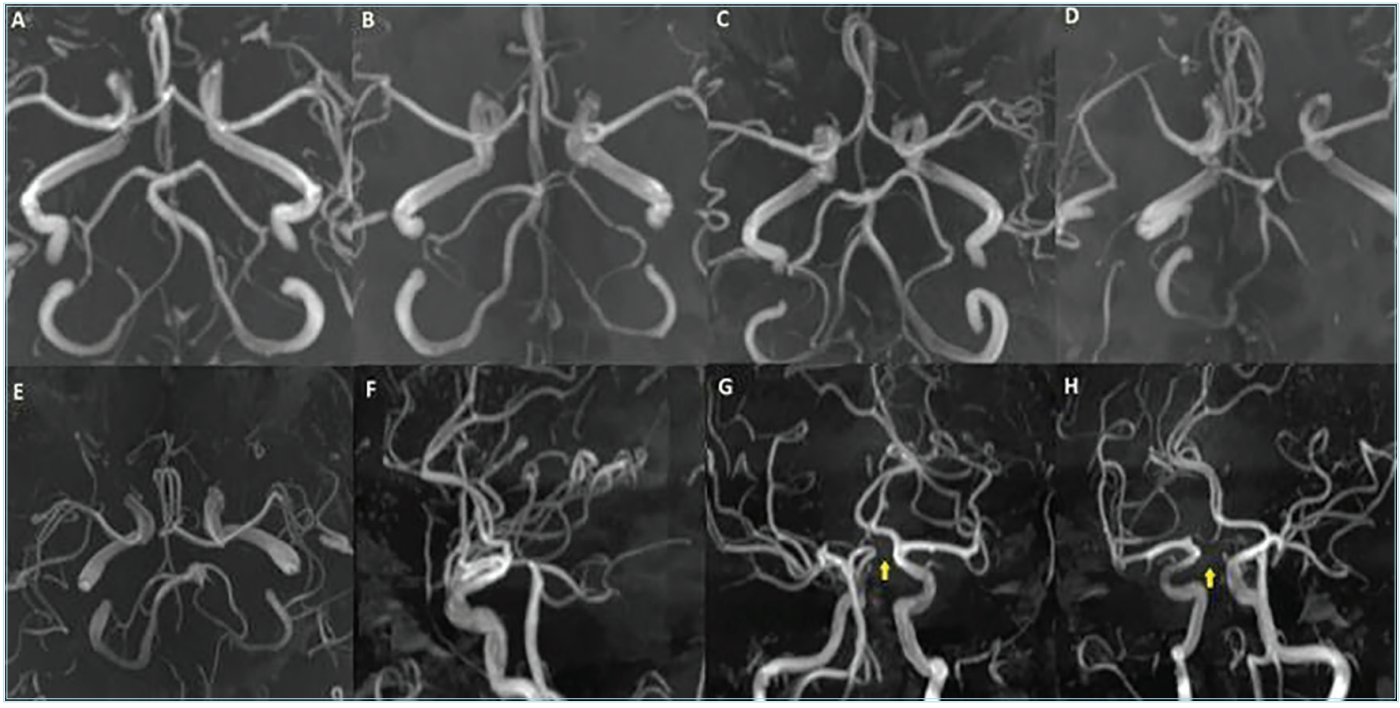

Figure 3. Some samples of MR angiography images from our patient population, classified as "partially incomplete" circle of Willis. The posterior circulation is characterized by the absence of both PComs (A). The posterior circulation is noted with the absence of the right PCom (B). Anterior circulation with anterior cerebral arteries originating from a common trunk (C). The anterior circulation is characterized by the absence of the left A1 segment (D). Another patient posterior circulation (E) and lateral (F), right oblique (G) and left oblique (H) images of the same patient indicate the absence of bilateral PComs (yellow arrows)

MR: Magnetic resonance, PCom: Posterior communicating artery

The high prevalence of PCom segment variations suggests greater embryological variability in the posterior circle.[14] These variations may reduce vertebrobasilar contributions to posterior circulation and help identify vulnerable regions in cerebrovascular events.[15]

Study Limitations

This study had limitations that should be noted. First, the 3D TOF sequence is not a perfect imaging technique for measuring vascular calibrations and analyzing them. Although this technique is widely used and very successful in imaging intracerebral circulation, it has some difficulties in imaging small vascular collateral channels because of turbulent flow, or slower velocity of blood adjacent to the vessel wall due to the laminar flow.

Conclusion

The COW exhibits significant anatomical variability between individuals. This study, using 1.5T TOF MRA, demonstrated that posterior segment

variations are particularly common. Awareness of these anatomical patterns is important in clinical decision-making, influencing treatment strategies and risk assessment.

Ethics

Ethics Committee Approval: The study was conducted with approval from the Erzincan Binali Yıldırım University Non-Interventional Clinical Research Ethics Committee (decision no: 2025-14/05, date: 24.07.2025).

Informed Consent: Since the study was a retrospective study, informed consent was not required by the ethics committee.

Footnotes

Authorship Contributions

Surgical and Medical Practices: K.B., Concept: K.B., M.S., Desing: K.B., Data Collection or Processing: K.B., M.S., Analysis or Interpretation: T.K., M.S., Literature Search: K.B., T.K., M.S., Writing: K.B., T.K., M.S.

Conflict of Interest: No conflict of interest was declared by the authors.

Financial Disclosure: The authors declared that this study received no financial support.

References

1. Kapoor K, Singh B, Dewan LI. Variations in the configuration of the circle of Willis. Anat Sci Int. 2008;83:96-106.
2. Alpers BJ, Berry RG, Paddıson RM. Anatomical studies of the circle of Willis in normal brain. AMA Arch Neurol Psychiatry. 1959;81:409-18.
3. Krabbe-Hartkamp MJ, van der Grond J, de Leeuw FE, Circle of Willis: morphologic variation on three-dimensional time-of-flight MR angiograms. Radiology. 1998;207:103-11.
4. Macchi C, Catini C, Federico C. Magnetic resonance angiographic evaluation of circulus arteriosus cerebri (circle of Willis): a morphologic study in 100 human healthy subjects. Ital J Anat Embryol. 1996;101:115-23.
5. Eftekhar B, Dadmehr M, Ansari S, Ghodsi M, Nazparvar B, Ketabchi E. Are the distributions of variations of circle of Willis different in different populations? -Results of an anatomical study and review of literature. BMC Neurol. 2006;6:22.
6. Chuang YM, Liu CY, Pan PJ, Lin CP. Posterior communicating artery hypoplasia as a risk factor for acute ischemic stroke in the absence of carotid artery occlusion. J Clin Neurosci. 2008;15:1376-81.
7. van Raamt AF, Mali WP, van Laar PJ, van der Graaf Y. The fetal variant of the circle of Willis and its influence on the cerebral collateral circulation. Cerebrovasc Dis. 2006;22:217-24.
8. Di Pietro M, Di Stefano V, Cannella R, Di Blasio F, De Angelis MV. Fetal variant of posterior cerebral artery: just a physiologic variant or a window for possible ischemic stroke? Neurol Sci. 2021;42:2535-8.
9. Hartkamp MJ, van Der Grond J, van Everdingen KJ, Hillen B, Mali WP. Circle of Willis collateral flow investigated by magnetic resonance angiography. Stroke. 1999;30:2671-8.
10. Giotta Lucifero A, Baldoncini M, Bruno N, et al. Microsurgical neurovascular anatomy of the brain: the anterior circulation (Part I). Acta Biomed. 2021;92(S4):e2021412.
11. Chen HW, Yen PS, Lee CC, et al. Magnetic resonance angiographic evaluation of circle of Willis in general population: A morphologic study in 507 cases. Chinese Journal of Radiology. 2004;29:223-9.
12. Shaban A, Albright KC, Boehme AK, Martin-Schild S. Circle of Willis variants: fetal PCA. Stroke Res Treat. 2013;2013:105937.
13. Coulier B. Morphologic variants of the cerebral arterial circle on computed tomographic angiography (CTA): a large retrospective study. Surg Radiol Anat. 2021;43:417-26.
14. Furuichi K, Ishikawa A, Uwabe C, Makishima H, Yamada S, Takakuwa T. Variations of the circle of Willis at the end of the human embryonic period. Anat Rec (Hoboken). 2018;301:1312-9.
15. Chandra A, Li WA, Stone CR, Geng X, Ding Y. The cerebral circulation and cerebrovascular disease I: Anatomy. Brain Circ. 2017;3:45-56.

RESEARCH ARTICLE

DOI: 10.4274/AdvRadiolImaging.galenos.2025.69775
Adv Radiol Imaging 2025;2(2):36-39

Does Foramen Magnum Based on Computed Tomography Measurements Change with Age and Gender?

Özlem Çelik Aydın[1], Esra Bilici[2], Mukadder Sunar[3]

[1]*Erzincan Binali Yıldırım University Faculty of Medicine, Department of Pharmacology, Erzincan, Türkiye*
[2]*Erzincan Binali Yıldırım University Faculty of Medicine, Department of Radiology, Erzincan, Türkiye*
[3]*Erzincan Binali Yıldırım University Faculty of Medicine, Department of Anatomy, Erzincan, Türkiye*

Abstract

Objectives: The aim of the study was to determine the development rate of foramen magnum (FM) with age by performing morphometric analysis of FM using computed tomography (CT) examination in children at different ages, accounting for sagittal and transverse dimensions for FM as well as sex.

Methods: Two hundred and fifty-one children aged 0-18, who had CT imaging at our institution for any reason between January and December 2024 had their anterior-posterior diameter and transverse diameter (TD) measured in this retrospective study. The information was statistically analyzed.

Results: The study included 251 children, 156 boys (62.2%) and 95 girls (37.8%). The mean sagittal diameter (SD) of all children was 36, and the mean TD was 29. Age, and SD and TD values had a substantial positive connection ($p<0.05$). There were no appreciable variations in SD and TD measurements between boys and girls at any age.

Conclusion: Morphometric research in anthropology aids in determining anthropometric variations among populations, which may be influenced by factors such as ethnicity, gender, age, and genetics, and may influence bone size and shape. Additionally, it can differentiate between a pathogenic situation and typical variations. For many abnormalities, it is essential to ascertain the size of FM and how it changes with age.

Keywords: Anthropology, morphometry, children, foramen magnum

Introduction

The entire occipital bone encloses the foramen magnum (FM), which joins the posterior fossa and the vertebral canal, ensuring interaction between the skull and the cervical vertebrae. Numerous biological fields, including anatomy, forensic medicine, and anthropology, are interested in studying FM.[1] Skull, FM morphology show sex-specific traits and can identify sex with 80% accuracy in anthropology and forensic medicine.[2] It is unknown how children's FM dimensions change as they get older.[3]

Morphometric measurements of a child's skull are used to evaluate the course of a disease or the effectiveness of treatment for certain developmental abnormalities, or skull deformities caused by various illnesses. Developmental variations in FM's size in response to the child's age are significant in these situations.

Anthropometric studies related to FM show differences according to gender, and studies conducted on skulls have proven that the transverse and sagittal dimensions of FM are higher in males than in females.[4] However, it is not known exactly how FM dimensions change as children age.[3]

Determining the average FM dimensions in children for each age group and based on gender[5] seems reasonable. The purpose of this study was to measure the sagittal and transverse dimensions of the FM using computed tomography (CT) examination in children of various ages, accounting for gender. This was done to perform a morphometric analysis and ascertain how the FM changes with age.

Methods

This study was approved by the Non-Interventional Clinical Research Ethics Committee of Erzincan Binali Yıldırım University (decision no: 417789, date: 03.01.2025). In this study, cranial CT images were obtained using a 128-slice multi-detector CT scanner with a slice thickness of 0.625 mm. The study's data came from re-examining the digital patient archives, to find images of 313 patients who had CT evaluations in our hospital between January and December 2024 for various reasons.

Cite this article as: Çelik Aydın Ö, Bilici E, Sunar M. Does foramen magnum based on computed tomography measurements change with age and gender? Adv Radiol Imaging. 2025;2(2):36-39

Address for Correspondence: Esra Bilici MD, Erzincan Binali Yıldırım University Faculty of Medicine, Department of Radiology, Erzincan, Türkiye
E-mail: esra.bilici@hotmail.com ORCID ID: orcid.org/0009-0007-9983-8901
Received: 29.06.2025 Accepted: 19.08.2025 Published: 29.08.2025

Since the study was conducted retrospectively, no additional informed consent was required beyond what was initially obtained.

Following a review of the image archives, 62 patients with image artifacts or trauma in the occipital bone region were excluded from the study, and a total of 251 patients without trauma and with good image quality and positioning were included.

The patients were children aged 0-18. In this descriptive study, patients were divided into age groups: 0-1 years, 2-4 years, 5-8 years, 9-13 years, and 14-17 years. The study comprised 251 patients.

A Vernier Caliper was used to measure the FM's anteroposterior and transverse transverse diameters (TD) with an accuracy of 0.1 mm (Figure 1). The distance in the mid-sagittal plane between the opisthion (posterior border) and the basion (anterior border) is known as the anteroposterior diameter (APD) of the FM. The maximum distance along the transverse plane is known as the TD.

Statistical Analysis

Statistical analysis of the measurements was performed. Data were analyzed using the Statistical Package for the Social Sciences (IBM SPSS 22.0, IBM Corporation®, Armonk, NY, USA) software (IBM SPSS Inc.). Values with $p<0.05$ were considered statistically significant.

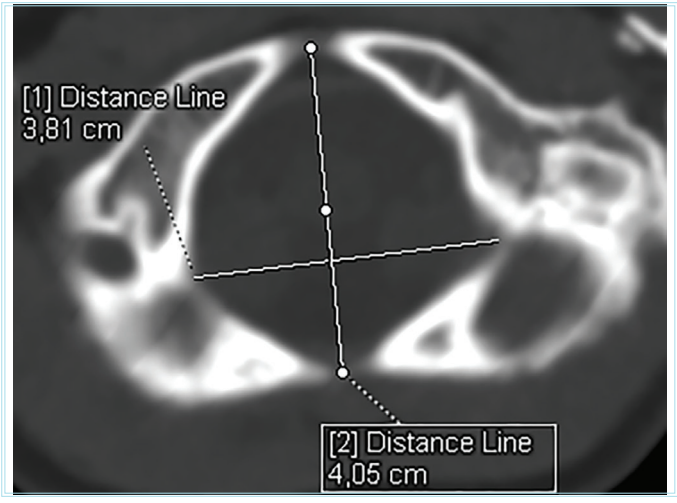

Figure 1. The widest transverse and longest sagittal length measurements of the axial plane foramen magnum were taken. The yellow arrow indicates the measurement of the longest sagittal diameter, while the blue arrow indicates the measurement of the widest transverse diameter

Results

The study included 251 children, 156 boys (62.2%) and 95 girls (37.8%). The youngest age included in the study was 2 months, and the oldest age was 17 years. The median age of children was 7.

The lowest sagittal diameter (SD) measurement value is 26, and the highest is 44. The lowest and highest SD values in girls were found to be 26 and 44, respectively, while in boys they were found to be 19 and 37. The mean SD of all children was 36 and the mean TD was 29.

In FM measurements, the sagittal dimension is greater than TD in all ages.

There was no discernible gender difference in any of the SD, TD measurement values between girls and boys.

Tables 1 and 2 display the general measurements and specific SD, TD values along with their values in boys and girls.

Compared to the other groups, all measurements made at ages 0-1 years and 2-4 years were noticeably lower. Measurements taken at ages 5-8 and 9-13, as well as 14-17, showed related results. At every age, there were no appreciable variations in SD and TD measurements between boys and girls.

Age and SD and TD values had a substantial positive connection ($p<0.05$). Table 3 provides a summary of the results.

Discussion

Morphometric research in anthropology aids in determining anthropometric variations among populations, such as ethnicity, gender, age, and genetic factors, that may influence bone size and shape. Additionally it can differentiate between a pathogenic situation and typical variations.[1] For many abnormalities, it is essential to ascertain the size of FM and how it changes with age.[5] In addition, knowing the size of the FM is important in diagnosing diseases such as FM meningioma, and in planning intracranial surgery.[6]

Adult measurements from imaging and dry skull investigations serve as the foundation for most FM evaluations.[7]

Table 1. The min. and max. values SD and TD values are shown

	Min. (mm)	Max. (mm)	Median
SD	26	44	36
TD	19	37	29

SD: Sagittal diameter, TD: Transverse diameter, Min.: Minimum, Max.: Maximum

Table 2. The results obtained for the sagittal and transverse dimensions of foramen magnum for the study group by sex

	Sex	Min. (mm)	Max. (mm)	Median
SD	Girl	27	41	34
	Boy	26	44	36
TD	Girl	20	35	29
	Boy	19	37	30

SD: Sagittal diameter, TD: Transverse diameter, Min.: Minimum, Max.: Maximum

Table 3. Changes in SD and TD values with age and gender

Age			SD			TD		
	Sex	N	Min.	Max.	Median	Min.	Max.	Median
0-1	Girl	18	27	39	32	20	34	24.5
	Boy	32	26	38	32	19	29	26
2-4	Girl	19	31	37	34	24	34	28
	Boy	34	30	39	36	24	33	28
5-8	Girl	21	35	40	37	27	33	30
	Boy	30	32	44	37	26	37	30
9-13	Girl	13	34	39	37	27	34	30
	Boy	30	33	42	38	26	36	31
14-17	Girl	24	34	42	37	27	35	30
	Boy	30	34	42	39	29	37	32

SD: Sagittal diameter, TD: Transverse diameter, Min.: Minimum, Max.: Maximum

More et al.[7] analyzed age groups and compared children in the 0-9 and 10-19 age groups using CT scans. In the 0-9 age group, the mean APD was 36.00 (SD 6.93) mm, and the mean TD was 27.85 (SD 0.64) mm. In the 10-19 age group, both dimensions were 35.70 (SD 3.38) mm and 29.45 (SD 2.86) mm. In our study, the mean SD was 34.6 and the mean TD was 27.6 in the 0-8 age group. In the 9-18 age group, the mean SD was 37.75 and the mean TD was 30.75.

Our study's mean FM SD and TD values compare to those found in adult research. Our findings were consistent with research by Ulcay et al.[8] in a Turkish population, where the mean SD was 35.81 mm and the TD was 28.14 mm.

The mean values of FM APD and TD presented in our study were similar to those reported by Ganapathy et al.[9] in their study of the Indian adult population. In their study, the mean SD value was 3.49±0.23, and the mean TD value was 2.98±0.25.

As in the studies conducted by Natsis et al.[10] on the Greek adult population, the study conducted by Osunwoke et al.[11] on the skulls of the African adult population also showed results close to ours.

In certain instances, the mean values we found in children were greater or less than the FM dimensions of adults.[6,7,12,13] The sample size, measuring technique, or racial disparities could all be to blame for the discrepancies in the reported data.

The mean values for girls and boys in the children's study by More et al.[7] were 35.15 (SD 3.76) mm and 36.09 (SD 4.64) mm, respectively. Girls had a mean TD of 28.53 (SD 3.25) mm, whereas boys had a mean TD of 29.6 (SD 3.49) mm. Our results and those obtained were comparable. Although the results are similar, the two studies show minor differences, which are likely due to population differences and the use of different age ranges.

Given the statistically significant results, the findings are compatible with Shepur et al.[12] claim that FM achieves its maximum size in early childhood.

As a result, in this study investigating changes in FM morphology with age and sex, no difference was observed in SD and TD measurements between girls and boys, while a positive correlation was found with age.

Study Limitations

Our study has some limitations. First, this study is retrospective, so a comprehensive data review and detailed history were not possible. Second, our small sample size limits statistical analysis and reduces the power of our results. Third, images containing artifacts could not be included in the study because data measurement was not possible.

Conclusion

The morphology and size measurement of the FM have been extensively studied in the literature, although the pediatric age group has received relatively little attention.

As a result, in this study investigating changes in FM morphology with age and gender, no difference was observed in SD and TD measurements between girls and boys, while a positive correlation was found with age.

Ethics

Ethics Committee Approval: This study was approved by the Non-Interventional Clinical Research Ethics Committee of Erzincan Binali Yıldırım University (decision no: 417789, date: 03.01.2025).

Informed Consent: Since the study was conducted retrospectively, no additional informed consent was required beyond what was initially obtained.

Footnotes

Authorship Contributions

Surgical and Medical Practices: E.B., M.S., Concept: Ö.Ç.A., Design: Ö.Ç.A., M.S., Data Collection or Processing: E.B., Analysis or Interpretation: Ö.Ç.A., Literature Search: E.B., M.S., Writing: E.B.

Conflict of Interest: No conflict of interest was declared by the authors.

Financial Disclosure: The authors declared that this study received no financial support.

References

1. Madadin M, Menezes RG, Al Saif HS, et al. Morphometric evaluation of the foramen magnum for sex determination: a study from Saudi Arabia. J Forensic Leg Med. 2017;46:66-71.
2. İlgüy D, İlgüy M, Ersan N, Dölekoğlu S, Fişekçioğlu E. Measurements of the foramen magnum and mandible in relation to sex using CBCT. J Forensic Sci. 2014;59:601-5.
3. Wilk R, Moroz M, Zięba K, Likus W. Foramen magnum morphometry in children based on computed tomography examination. Folia Morphol (Warsz). 2023;82:587-95.
4. Pires LAS, Teixeira A, de Oliveira Leite TF, Babinski MA, Chagas CA. Morphometric aspects of the foramen magnum and the orbit in Brazilian dry skulls. Int J Med Res Health Sci. 2016;5:34-42.
5. Furtado SV, Thakre DJ, Venkatesh PK, Reddy K, Hegde AS. Morphometric analysis of foramen magnum dimensions and intracranial volume in pediatric Chiari I malformation. Acta Neurochir (Wien). 2010;152:221-7.
6. Campero A, Baldoncini M, Villalonga JF, Paíz M, Giotta Lucifero A, Luzzi S. Transcondylar fossa approach for resection of anterolateral foramen magnum meningioma: 2-dimensional operative video. World Neurosurg. 2021;154:91-2.
7. More CB, Saha N, Vijayvargiya R. Morphological analysis of foramen magnum for gender determination by using computed tomography. J Oral Med Oral Surg Oral Pathol Oral Radiol. 2015;1:51-6.
8. Ulcay T, Kamaşak B, Görgülü Ö, Uzun A, Aycan K. A golden ratio for foramen magnum: an anatomical pilot study. Folia Morphol (Warsz). 2022;81:220-6.
9. Ganapathy A, T S, Rao S. Morphometric analysis of foramen magnum in adult human skulls and CT images. Int J Cur Res Rev. 2014;6:11-5.
10. Natsis K, Piagkou M, Skotsimara G, Piagkos G, Skandalakis P. A morphometric anatomical and comparative study of the foramen magnum region in a Greek population. Surg Radiol Anat. 2013;35:925-34.
11. Osunwoke E, Oladipo G, Gwunireama IU. Morphometric analysis of the foramen magnum and jugular foramen in adult skulls in southern Nigerian population. Am J Sci Ind Res. 2012;3:446-8.
12. Shepur MP, M M, B N, Havaldar PP, Gogi P, Saheb SH. Morphometric analysis of foramen magnum. Int J Anat Res. 2014;2:249-55.
13. Chethan P, Prakash KG, Murlimanju BV, et al. Morphological analysis and morphometry of the foramen magnum: an anatomical investigation. Turk Neurosurg. 2012;22:416-9.

RESEARCH ARTICLE

DOI: 10.4274/AdvRadiolImaging.galenos.2025.54254
Adv Radiol Imaging 2025;2(2):40-44

An Update on Cardiothoracic Ratio: A Study of X-Ray Measurements

Berihat Kızılgöz[1], Muhammet Fırat Öztepe[2]

[1]*Republic of Türkiye Ministry of Health, Provincial Health Directorate, Community Health Center, Erzincan, Türkiye*
[2]*Erzincan Binali Yıldırım University Faculty of Medicine, Department of Radiology, Erzincan, Türkiye*

Abstract

Objectives: The aim of the study was to reveal the mean values of the cardiothoracic ratio (CTR) and the effect of gender and age on these measurements performed on chest radiographies.

Methods: After the exclusion of positive findings on radiographic images and the findings compatible with cardiovascular disease, the radiographies of 277 patients were re-evaluated regarding CTR measurements on chest X-rays. The maximum interval of the right and left heart borders, along with the horizontal thoracic diameter, were measured.

Results: The mean values of CTR were 0.45±0.02, 0.46±0.02 and 0.44±0.02 for the total study population, for the female group, and the male group respectively. Higher CTR was measured for females than for males ($p<0.001$). Age indicated a low but significant positive correlation with the CTR for the total study population ($p<0.001$).

Conclusion: Chest X-ray is a fast and inexpensive imaging method; performing CTR measurements is very easy to apply on chest X-rays. CTR still serves as a significant indicator of cardiovascular diseases along with other important parameters observed in chest radiographs.

Keywords: Cardiothoracic ratio, chest X-rays, heart, age, gender

Introduction

Chest X-ray examination constitutes an important part of the diagnostic process for many physicians. Pulmonary parenchyma, airways, and vessels, mediastinum, heart, chest wall, and pleura can be evaluated with chest X-rays.[1] This imaging modality quickly provides the first impression of cardiothoracic diseases, and chest radiographies obtained via posteroanterior X-ray projection are a part of routine examinations for general practitioners and for specialists across all branches of clinicians and surgeons.

Cardiothoracic ratio (CTR) expresses the relationship between the transverse size of the heart and the transverse diameter of the chest measured on chest X-rays. It is a commonly used parameter in the evaluation of cardiomegaly with a threshold value of 0.5, and a value greater than 0.5 should be interpreted as enlargement of the heart.[2]

In this study, the investigators aimed to contribute to the literature with an update of CTR values and the influence of gender and age on this parameter for adult patients who had no pathologies indicated on the chest X-ray images or any known pathological cardiothoracic condition.

Methods

This study was approved by the Erzincan Binali Yıldırım University, Ethics Committee of Clinical Research approval (decision no: 2025-12/02, date: 17.07.2025). The requirement for informed consent from each patient participating in the study has been waived by the ethics committee based on the research methodology. All patients who had undergone chest X-ray imaging between the 1st and the 30th of June 2025 in the ambulatory care rooms were scanned. There were 350 patients listed on the picture archiving and communication system (PACS) of our hospital. The study aimed to measure the CTR of the adult individuals; therefore, the patients under 18 years old (n=5) were excluded. Patients with consolidation (n=8), atelectasis (n=14), lung nodule or mass (n=3), mediastinal mass (n=9), pericarditis (n=1), pleural effusions (n=4), scoliosis (n=3), and any cardiac or thoracic operation (n=14), were excluded. Additionally, suboptimal radiographs and X-rays with technical errors (such as inadequate patient positioning, dosage, or patient inspiration) (n=12) were not included. Cysts, cavities, bronchiectasis, interstitial lung disease, and vertebral or costal fractures were also planned to be excluded from the study; however, there were no patients with these findings in the study group. After the exclusions,

Cite this article as: Kızılgöz B, Öztepe MF. An update on cardiothoracic ratio: a study of X-ray measurements. Adv Radiol Imaging. 2025;2(2):40-44

Address for Correspondence: Berihat Kızılgöz MD, Republic of Türkiye Ministry of Health, Provincial Health Directorate, Community Health Center, Erzincan, Türkiye
E-mail: berihatkizilgoz@gmail.com **ORCID ID:** orcid.org/0009-0007-4986-2428
Received: 14.08.2025 **Accepted:** 22.08.2025 **Published:** 29.08.2025

chest X-rays of 277 patients were included in the study (Figure 1). Chest X-ray examinations were performed using the Samsung XGEO GC80/GC80V series. On the posteroanterior projection chest X-rays, the CTR is measured as the ratio of the greatest transverse dimension of the heart [addition of the maximum distance of the right heart border to the midline (a) and the maximum interval of the left heart border to the midline (b)] to the greatest transverse diameter of the chest cavity measured between the inner surfaces of the ribs (c) (Figure 2). The a and b values were recorded in millimeters. All measurements were performed by a radiology specialist with 8 years of experience. A PACS (Akgün PACS Viewer v7.5, Akgün Software, Ankara, Türkiye) was used for re-evaluation of the chest X-rays and to perform CTR measurements in standard digital imaging communications in medicine formats.

Statistical Analysis

All statistical calculations of the research were performed using IBM Statistical Package for the Social Sciences Statistics for Windows version 22.0 (IBM Corp., Armonk, NY, USA). The Kolmogorov-Smirnov test was used to analyze the distribution characteristics. The histogram graphics were used to present the data distribution of CTR measurement results for the total study population, females and males. After the data analysis, a normal data distribution could not be reached, therefore, a non-parametric test (Mann Whitney-U) was carried out to assess the significance of the difference between the female and the male group regarding CTR values. The correlation between age and all the other parameters of the study was calculated using Spearman's Rho test. Independent samples T-tests were carried out to reveal the difference between genders for the other parameters (a, b, c, and a+b). For all the statistical calculations, p values of <0.05 were considered to indicate statistical significance.

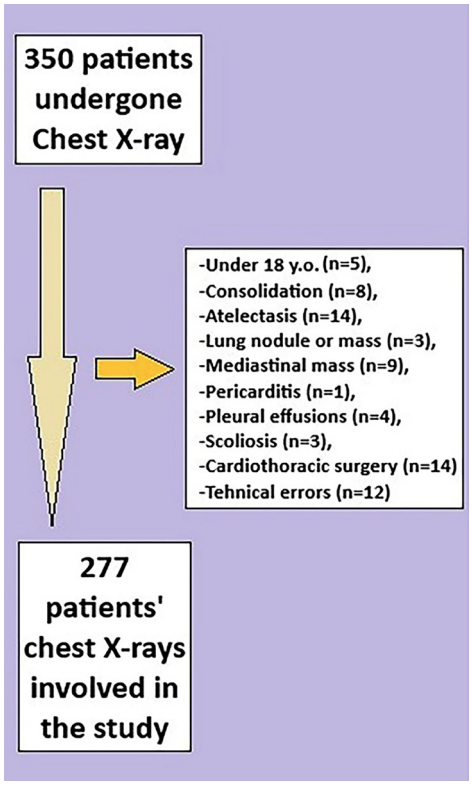

Figure 1. The workflow of the study

Results

Radiographies of 128 female and 149 male patients, totaling 277 patients, radiographies were re-evaluated regarding CTR measurements on chest X-rays. The mean age of the study population was 46.53±17.48. There was a significant difference between the female and male groups ($p<0.001$) regarding age (Table 1).

The data distribution was analyzed by the Kolmogorov-Smirnov test for the total study population, females, and the male group. The a, b, c, and a+b values indicated a normal data distribution, while a normal data distribution was not observed regarding age and the CTR values. The data distribution results were shown by boxplot analyses (Figure 3).

The male group showed higher a, b, a+b, and c values than females ($p=0.002$, $p<0.001$, $p<0.001$, and $p<0.001$, respectively) according to statistical calculations. Higher CTR values were reached for women compared to those of men in the study population ($p<0.001$) (Table 2).

Age indicated a significant positive and low correlation with b value, a+b value, and the CTR for the total study population ($p<0.001$ for each parameter). A significant, positive and moderate correlation was observed between age and the CTR for the female group ($p<0.001$), Age also showed a significant, positive, and moderate correlation with the a+b value in the male group ($p<0.001$) (Table 3).

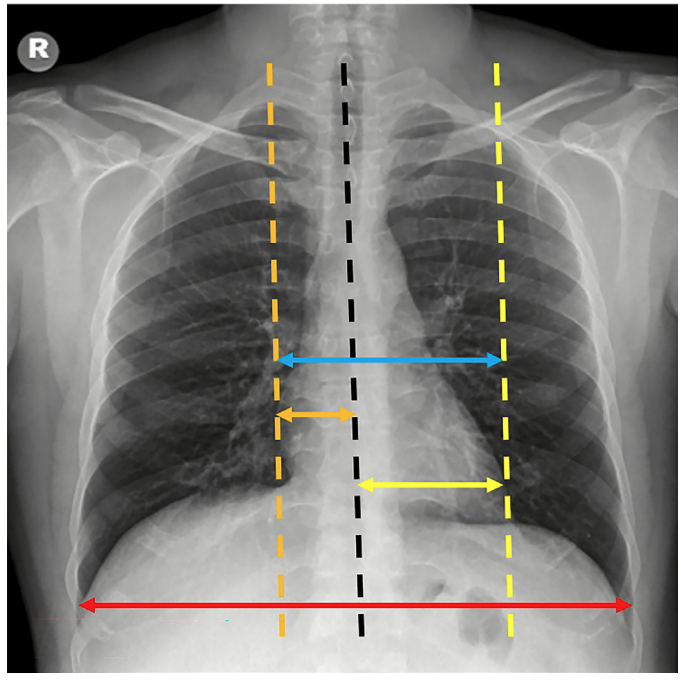

Figure 2. The dashed black line represents the midline in the radiograph. The orange line shows the maximum distance of the right heart border to the midline (a). The yellow line indicates the maximum distance from the left heart border to the midline (b). The red line shows the maximum transverse diameter of the chest cavity measured between the inner surfaces of the ribs (c). Cardiothoracic ratio is measured as (a+b)/(c)

Table 1. Demographic data of the study population

Gender (n)		Number		Percentage	
Females		128		46.2%	
Males		149		53.8%	
Total		277		-	
Age	**Mean**	**SD**	**Min.**	**Max.**	**p**
Females	50.57	16.56	18	88	<0.001
Males	43.07	17.55	18	81	
Total	46.53	17.48	18	88	-

SD: Standard deviation, Min.: Minimum, Max.: Maximum

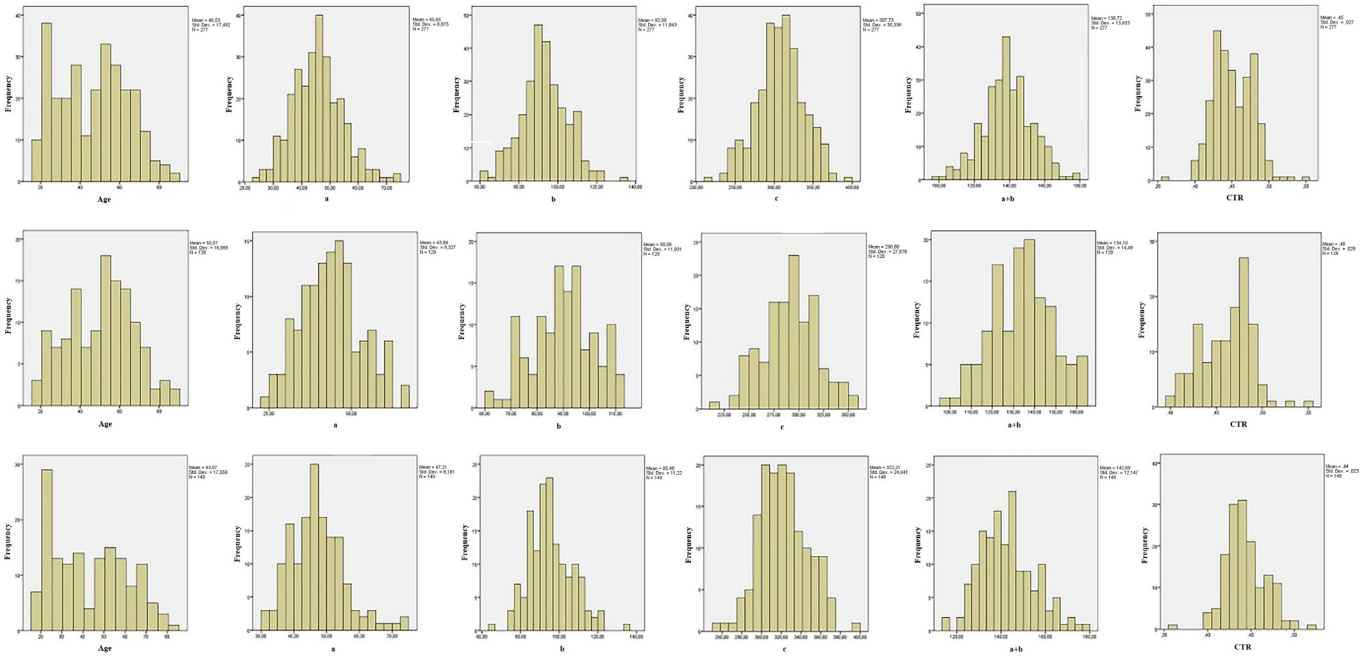

Figure 3. The histogram analysis for every measured parameter of the study. The upper, the middle and the lower row indicates the results for the total study population, the female group and the male group respectively. Normal data distribution could not be reached according to the Kolmogorov-Smirnov test regarding age and cardiothoracic ratio

Discussion

A well-obtained chest X-ray film should be observed with adequate penetration (vertebral bodies should be seen behind the heart to T7), no rotation (medial ends of clavicles should be equidistant from the vertebral spinous processes), and adequate inspiration (five to seven anterior ribs above the hemidiaphragm line). In a posteroanterior projection chest X-ray, the beam enters the chest posteriorly and the plate (detector) is located anterior to the patient. For ambulatory patients, radiographs were usually obtained in the standing position. As the heart is an anterior structure in the thorax, minimal magnification of the heart size is expected. The heart occupies less than half of the CTR, and cardiomegaly may be assumed when the ratio is greater than 50%. This assumption should not be made on any anteroposterior chest X-rays. In a normal chest X-ray, the right and left borders of the heart should be traced to make certain that there is no underlying pathological condition.[3] Heart diseases may be suspected with cardiomegaly (a CTR greater than 50%), with microcardia (a CTR less than 42%) or without an abnormality in shape or size of the heart.[4,5] On the other hand, anteroposterior radiographs have different geometries based on the X-ray projection. Based on the results of their work, Kabala and Wilde[6] proposed a 55% threshold to indicate the enlarged heart silhouette on anteroposterior radiographs. In their study, the width of the heart silhouette >165 mm for men and >150 mm for women is a significant indicator to exclude individuals with heart failure with a sensitivity of 92% and a specificity of 96%.

CTR is not only used to assess the cardiac size, but also for other significant purposes in medicine. A prospective study conducted with almost 3436 participants and a four-year follow-up revealed that an increased CTR is linked to an elevated risk (for both all-cause mortality and cardiovascular disease events) for individuals undergoing hemodialysis.[7] Hsu et al.[8] conducted a study on 186 patients undergoing hemodialysis and reported that CTR was higher in patients with vitamin D deficiency than in those without deficiency. In another study by Jiang et al.[9], the CTR is reported as a prognostic factor to predict poor outcomes in the patient group with rheumatic heart disease who have undergone valve replacement surgery. A CTR higher than 0.50 was found

to be associated with increased mortality and morbidity in outpatients with chronic heart failure.[10]

The mean value of the CTR was found to be 47.1%±3.7, and females had a significantly higher CTR than males (p=0.001) in a study by Brakohiapa et al.[11] In the current study, the measurement results for the CTR were 0.45±0.02, 0.46±0.02 and 0.44±0.02 for the total study population, for the female group and the male group, respectively. Moreover, a higher CTR was measured in females than in males, parallel to Brakohiapa et al.[12] study. In our research, a, b, a+b, and c values were also studied as distinct parameters and higher values were observed in males than in females. The study results might indicate higher cardiac dimensions in males. However, a higher horizontal chest diameter in men may explain the lower CTRs in the male group. Age was another parameter studied in the current research and showed a significant, positive, and low correlation with the b value, a+b value, and the CTR for the total study population. An increase in transverse cardiac diameter of 1 cm resulted in a CTR of greater than 0.50, in all patients except for males aged 21-40 years.

Table 2. The comparison between females and males regarding a, b, a+b, c and the CTR measurement results

	Mean	SD	p value
a value (mm)			
Females	43.83	9.32	0.002
Males	47.21	8.18	
Total	46.53	17.48	-
b value (mm)			
Females	90.09	11.93	<0.001
Males	95.47	11.21	
Total	92.98	11.84	-
c value (mm)			
Females	290.88	27.57	<0.001
Males	322.20	24.64	
Total	307.73	30.33	-
a+b value (mm)			
Females	134.09	14.49	<0.001
Males	142.68	12.14	
Total	138.72	13.93	-
CTR			
Females	0.46	0.02	<0.001
Males	0.44	0.02	
Total	0.45	0.02	-

a value: Maximum distance of the right heart border to the midline, b value: Maximum distance of the left heart border to the midline, c value: The maximum transverse diameter of the chest cavity measured between the inner surfaces of the ribs
SD: Standard deviation, CTR: Cardiothoracic ratio

Study Limitations

There are some aspects of this research that are limitations of the study. Even though the outpatients were chosen for the research, and the pathological cardiothoracic conditions were excluded from the statistical calculations, volunteers without symptoms of disease would be more suitable for reaching the normative mean values and ranges of the CTR. Moreover, some of the patients had not undergone a full cardiothoracic examination or relevant laboratory tests. There were patients referred to radiology from various departments of the hospital. The results showed a significant age difference between the female and the male groups. The females were older than the males in the study population. This situation might also influence the outcome of the study. Although the study was conducted on a relatively crowded population, a larger sample size would possibly reflect the normative values better.

Conclusion

To conclude, the chest X-ray is a fast and inexpensive imaging method that allows physicians to obtain rapid information about the presence of an underlying pathology. All doctors , including general practitioners, often use this modality to check the cardiothoracic conditions of patients quickly. Performing the measurements is very easy on chest X-rays, and the CTR still serves as a surrogate marker for the cardiovascular system along with other significant parameters from chest X-rays.

Table 3. The correlation analysis between age and five measured parameters (a, b, c, a+b and the CTR) for the total study population, the female group and the male group

		Total (n=277)	Female (n=128)	Male (n=149)
a value	Correlation coefficient	0.077	0.153	0.098
	p value	0.199	0.085	0.236
b value	Correlation coefficient	0.250	0.298	0.356
	p value	<0.001	0.001	<0.001
c value	Correlation coefficient	0.072	0.152	0.315
	p value	0.232	0.086	<0.001
a+b value	Correlation coefficient	0.283	0.351	0.427
	p value	<0.001	<0.001	<0.001
CTR	Correlation coefficient	0.392	0.461	0,260
	p value	<0.001	<0.001	0.001

a value: Maximum distance of the right heart border to the midline, b value: Maximum distance of the left heart border to the midline, c value: The maximum transverse diameter of the chest cavity measured between the inner surfaces of the ribs
CTR: Cardiothoracic ratio

Ethics

Ethics Committee Approval: This study was approved by the Erzincan Binali Yıldırım University, Ethics Committee of Clinical Research approval (decision no: 2025-12/02, date: 17.07.2025).

Informed Consent: The requirement for informed consent from each patient participating in the study has been waived by the ethics committee based on the research methodology.

Footnotes

Authorship Contributions

Surgical and Medical Practices: M.F.Ö., Concept: B.K., Design: B.K., Data Collection or Processing: B.K., M.F.Ö., Analysis or Interpretation: B.K., M.F.Ö., Literature Search: B.K., M.F.Ö., Writing: B.K.

Conflict of Interest: No conflict of interest was declared by the authors.

Financial Disclosure: The authors declared that this study received no financial support.

References

1. Speets AM, van der Graaf Y, Hoes AW, et al. Chest radiography in general practice: indications, diagnostic yield and consequences for patient management. Br J Gen Pract. 2006;56:574-8.
2. Truszkiewicz K, Poręba R, Gać P. Radiological cardiothoracic ratio in evidence-based medicine. J Clin Med. 2021;10:2016.
3. Bansal T, Beese R. Interpreting a chest X-ray. Br J Hosp Med (Lond). 2019;80:C75-9.
4. Morales MA, Prediletto R, Rossi G, Catapano G, Lombardi M, Rovai D. Routine chest X-ray: still valuable for the assessment of left ventricular size and function in the era of super machines? J Clin Imaging Sci. 2012;2:25.
5. Fonseca C, Mota T, Morais H, et al. The value of the electrocardiogram and chest X-ray for confirming or refuting a suspected diagnosis of heart failure in the community. Eur J Heart Fail. 2004;6:807-12, 821-2.
6. Kabala JE, Wilde P. The measurement of heart size in the antero-posterior chest radiograph. Br J Radiol. 1987;60:981-6.
7. Yotsueda R, Taniguchi M, Tanaka S, et al. Cardiothoracic ratio and all-cause mortality and cardiovascular disease events in hemodialysis patients: the q-cohort study. Am J Kidney Dis. 2017;70:84-92.
8. Hsu HJ, Wu IW, Hsu KH, Sun CY, Chen CY, Lee CC. Vitamin D deficiency, cardiothoracic ratio, and long-term mortality in hemodialysis patients. Sci Rep. 2020;10:7533.
9. Jiang L, Chen WG, Geng QS, et al. The cardiothoracic ratio: a neglected preoperative risk-stratified method for patients with rheumatic heart disease undergoing valve replacement surgery. Eur J Cardiothorac Surg. 2019;55:511-7.
10. Giamouzis G, Sui X, Love TE, Butler J, Young JB, Ahmed A. A propensity-matched study of the association of cardiothoracic ratio with morbidity and mortality in chronic heart failure. Am J Cardiol. 2008;101:343-7.
11. Brakohiapa EK, Botwe BO, Sarkodie BD. Gender and age differences in cardiac size parameters of ghanaian adults: can one parameter fit all? Part two. Ethiop J Health Sci. 2021;31:561-72.
12. Brakohiapa EKK, Botwe BO, Sarkodie BD, Ofori EK, Coleman J. Radiographic determination of cardiomegaly using cardiothoracic ratio and transverse cardiac diameter: can one size fit all? Part one. Pan Afr Med J. 2017;27:201.